T. Magn. Soc. Jpn. (Special Issues)., **1**, 30-33 (2017)

<Paper>

Fabrication and magnetic properties of $L1_0$-MnGa highly oriented thin films

Y. Takahashi, H. Makuta, T. Shima and M. Doi

Graduate School of Engineering, Tohoku Gakuin University, Tagajo 980-8573, Japan

$L1_0$-Mn-Ga highly oriented thin films were prepared on MgO (100) single crystalline substrates with a Cr buffer layer using an ultra-high-vacuum electron beam vapor deposition system. All growths are monitored in real-time using reflection high-energy electron diffraction (RHEED). The RHEED pattern shows clear oriented growth. In addition, XRD patterns for a fundamental (002) peak and (001) and (003) superlattice peaks were clearly observed. Large magnetic anisotropy (K_u) of 10.5 Merg/cm^3 and saturation magnetization (M_s) of 470 emu/cm^3 were observed for $L1_0$-Mn-Ga film (100 nm) at T_s = 300 ℃. When the thickness of $L1_0$-Mn-Ga decreased from 100nm to 5nm, K_u (= 6.01 Merg/cm^3), M_s (= 302 emu/cm^3) and R_a (= 1.45 nm) were decreased, respectively.

Keywords: $L1_0$-Mn-Ga, magnetic anisotropy, saturation magnetization, electron beam evaporation method, thin film

1. Introduction

Mn-Ga alloy thin film is known to exhibit a saturation magnetization; M_s ~ 200-600 emu/cm^3 [1, 2, 5], a high magnetic anisotropy; K_u ~ 10-23.5 Merg/cm^3 [1], a high spin polarization; P ~ 88 % (it was theoretically predicted to be a half-metallic-like ferrimagnet) [3] and 58 % experimentally [4], and a low Gilbert damping constant; α ~ 0.008-0.015 [1]. It has been attractive attention as a new material for spin electronics device [5-12]. Recently, thin films of ordered Mn-Ga alloy is one of the most intensively studied materials for a magnetic tunnel junction (MTJ) for the super gigabit (Gbit) class magnetic random access memory operated by spin transfer torque (STT-MRAM) [14-20]. The primary issue to be addressed in MRAM applications is to reduce the critical current (I_c) required for STT-induced magnetization switching. Therefore, MTJ films should have a low M_s ~ 100 emu/cm^3, a low α ≦ 0.01, a high K_u ≧ 10 Merg/cm^3, and a high P ≧ 70 %, Mn-Ga alloy thin film is very attractive to satisfy these required properties [13]. In addition, the thickness of the magnetic free layer in such STT device is required to be below 5nm in general [10]. At the moment, little has been reported on $L1_0$-MnGa thin film having a high perpendicular magnetic anisotropy (PMA) oriented perpendicular to the substrate by using an ultra high vacuum electron beam (UHV-EB) vapor deposition system.

In this paper, $L1_0$-MnGa highly oriented thin films have been fabricated by using an UHV-EB vapor deposition system and their magnetic properties ware investigated.

2. Experimental procedure

Prior to film deposition, $Mn_{1.0}Ga$ target alloys were prepared from high purity manganese (99.999 %) and gallium (99.9999 %) by arc melting method in argon atmosphere. The base pressure of arc melting was less than 10^{-3} Pa. Mn-Ga thin films were prepared on MgO (100) single crystalline substrates with a Cr buffer layer using an ultra-high-vacuum electron beam evaporation system with a base pressure below 8.9×10^{-7} Pa. The stacking structure of sample was follows: MgO (100) substrate/ Cr (5 nm)/ Mn-Ga (100-5 nm)/ Cr (10 nm). The substrate was heated to T_a = 300 ℃ during deposition and annealed at 300 ℃ (3 h) for improve the quality of crystal. The compositions of the films were determined by an energy dispersive X-ray spectroscopy (EDX) and X = 77.8 (1st depo.), 71.5 (2nd depo.), 62.0 (3rd depo.), 69.9 (4th depo.), 59.3 (5th depo.) and 44.6 (6th depo.) for Mn_XGa_{100-X} (at. %) are confirmed. All growths are monitored in real-time using reflection high-energy electron diffraction (RHEED). The crystal structure of the samples was characterized by X-ray diffraction (XRD) with the Cu Kα radiation line

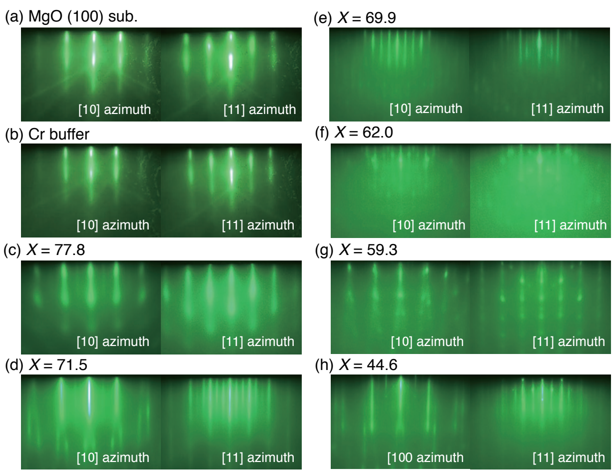

Fig. 1. RHEED patterns for the substrate, buffer and Mn_XGa_{100-X} thin films at T_s = 300 ℃. (a) MgO (100) sub., (b) Cr buffer, (c) 77.8, (d) 71.5, (e) 69.9, (f) 62.0, (g) 59.3, (h) 44.6 with the electron beam azimuth [10] and [11] of MgO (100) substrate.

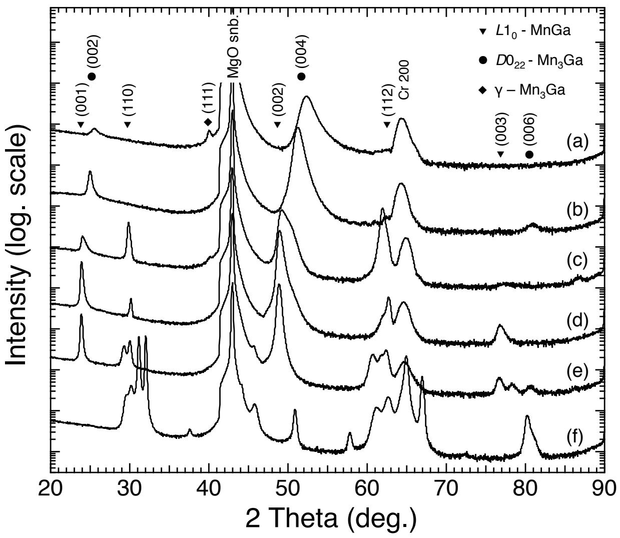

Fig. 2. XRD patterns for MnGa thin films prepared on MgO (100) substrate at T_s = 300 ℃. The Mn content X for Mn_XGa_{100-X} films (100 nm) are (a) 77.8, (b) 71.5, (c) 69.9, (d) 62.0, (e) 59.3 and (f) 44.6 (at. %).

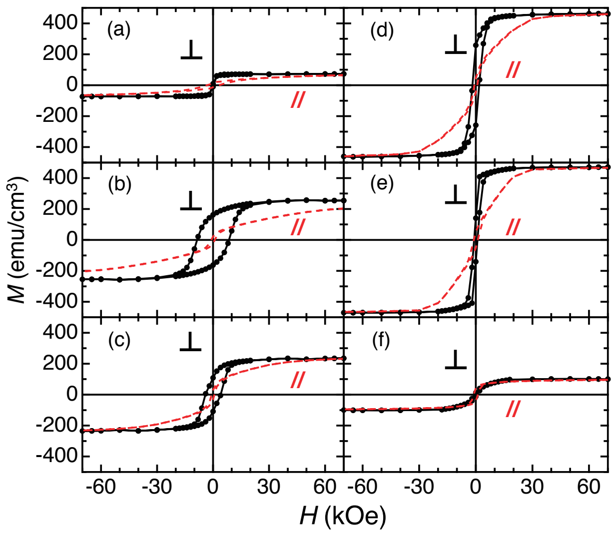

Fig. 3. Magnetization curves for MnGa thin films prepared on MgO (100) substrate at T_s = 300 ℃. The Mn content X for Mn_XGa_{100-X} films (100 nm) are (a) 77.8, (b) 71.5, (c) 69.9, (d) 62.0, (e) 59.3 and (f) 44.6 (at. %).

(wavelength equal to 0.15418 nm). The surface roughness of the film was investigated by atomic force microscopy (AFM). The magnetic properties were measured by using a superconducting quantum interference device (SQUID) magnetometer in the field up to ±70 kOe, and M_s and K_u for each thin film were evaluated from magnetization curves.

3. Results and discussion

RHEED patterns of Cr buffer and the growth of Mn_XGa_{100-X} films (100 nm) with various Mn content prepared on MgO (100) substrate are shown in Fig.1. The Mn content was varied as follows: X = (a) 77.8, (b) 71.5, (c) 69.9, (d) 62.0, (e) 59.3 and (f) 44.6 (at. %). The Mn_XGa_{100-X} films were fabricated from only $Mn_{1.0}Ga$ target alloy. The RHEED pattern shows clear oriented growth in c-plane, and the surface reconstruction structure in Mn-Ga layer was clearly observed. It should be noted that this oriented thin film exhibits a flat surface at the atomic level.

Since the composition is different by number of deposition by vapor pressure difference, Mn-Ga films were confirmed that it is a $L1_0$ structure by using XRD. XRD patterns for Mn_XGa_{100-X} films with various Mn content prepared on MgO (100) substrate are shown in Fig. 2. The Mn content was varied as follows: X = (a) 77.8, (b) 71.5, (c) 69.9, (d) 62.0, (e) 59.3 and (f) 44.6 (at. %). The intense peak from Cr buffer layer and MgO substrate ware clearly observed for all sample. In addition, a fundamental (002) peak, (001) and (003) superlattice peaks of the $L1_0$-MnGa phase were clearly observed for X = 62.0 (at. %) (d) and X = 59.3 (at. %) (e). Furthermore, both fundamental (004) and superlattice (002) and (006) peaks of the $D0_{22}$-Mn_3Ga phase were confirmed at the X = 71.5 (at. %) (b). The chemical order parameter S of X = 62.0 (at. %) (d) and X = 59.3 (at. %) (e) were shown S = 0.79 and 0.86. However, Mn-Ga thin film of X = 59.3 (at. %) (e) show decrease of (003) superlattice peak of the $L1_0$-MnGa phase. Therefore, the Mn-Ga thin film of X = 62.0 (at. %) (d) shows best preferred orientation of $L1_0$ structure.

Magnetization curves for the Mn_XGa_{100-X} films prepared on MgO (100) substrate are shown in Fig. 3. All measurements were preformed at room temperature. A magnetic field was applied perpendicular to the film plane direction for the curves indicated by ⊥, and it was applied along the in-plane direction for those indicated by //. Magnetization curve for X = 71.5 (at. %) (b) shows the curve of the case of a typical $D0_{22}$ structure [2,12]. Moreover, Mn-Ga films of X = 62.0 (at. %) (d) and X = 59.3 (at. %) (e) had relatively high M_s and low H_c. To evaluate the PMA properties quantitatively, the K_u was

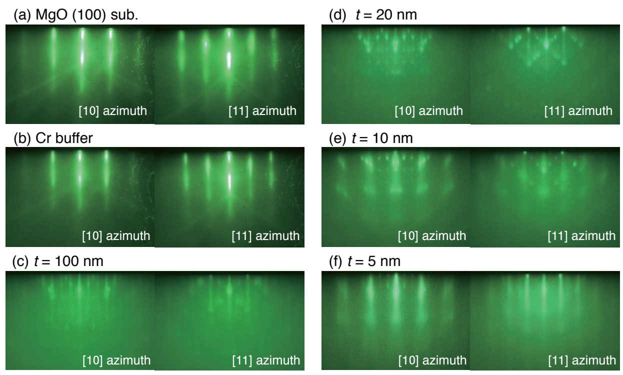

Fig. 4. RHEED patterns for the substrate, buffer and $Mn_{62.0}Ga_{38.0}$ (at %) thin films of different thickness ($t_{Mn\text{-}Ga}$ nm) at T_s = 300 ℃. (a) MgO (100) sub., (b) Cr buffer, (c) 100, (d)20, (e)10, (f)5 with the electron beam azimuth [10] and [11] of MgO (100) substrate.

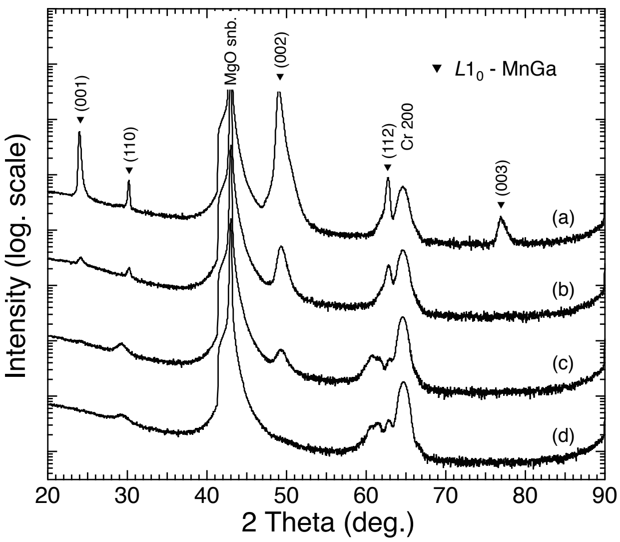

Fig. 5. XRD patterns for $Mn_{62.0}Ga_{38.0}$ (at %) thin films of different thickness ($t_{Mn\text{-}Ga}$ nm) prepared on MgO (100) substrate. $t_{Mn\text{-}Ga}$ of (a) 100, (b) 20, (c) 10 and (d) 5 at T_s = 300 ℃ and T_a = 300 ℃ (3 h).

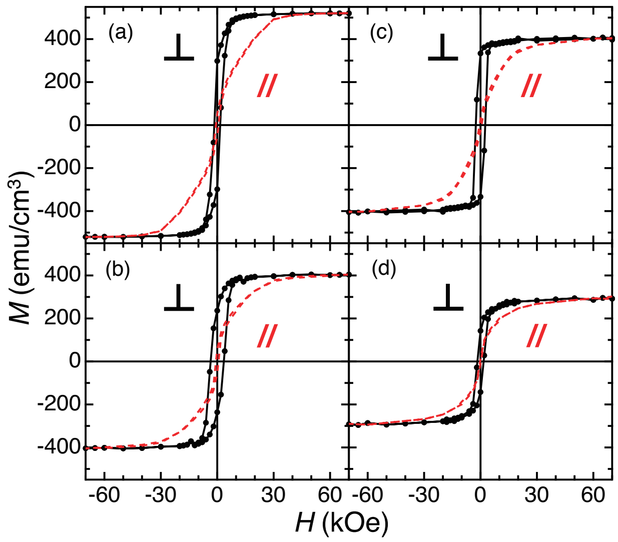

Fig. 6. Magnetization curves for $Mn_{62.0}Ga_{38.0}$ (at %) thin films of different thickness ($t_{Mn\text{-}Ga}$ nm) prepared on MgO (100) substrate. $t_{Mn\text{-}Ga}$ of (a) 100, (b) 20, (c) 10 and (d) 5 at T_s = 300 ℃ and T_a = 300 ℃ (3 h).

estimated using the relations $K_u = M_s \times H_k^{eff} / 2 + 2\pi M_s^2$. Here, the effective anisotropy field (H_k^{eff}) was defined as the extrapolated intersection of the in-plane M-H curves with the saturation magnetization value of out-of-plane M-H curves. In Mn-Ga films of X = 71.5 (at. %) (b), X = 62.0 (at. %) (d) and X = 59.3 (at. %) (e), Mn-Ga films with high $K_u \geqq$ 10 Merg/cm³ were obtained. Highest M_s of 470 emu/cm³ and K_u of 10.5 Merg/cm³ were confirmed by epitaxial Mn-Ga film of X = 62.0 (at. %) (d).

RHEED patterns of Cr buffer and the growth of $Mn_{62.0}Ga_{38.0}$ (at %) films of different thickness ($t_{Mn\text{-}Ga}$ nm) on MgO (100) substrate are shown in Fig.4, $t_{Mn\text{-}Ga}$ is (c) 100, (b) 20, (c) 10 and (d) 5. The observed RHEED patterns remain somehow bright and streaky. This indicates that the films are highly crystalline and have rough surfaces except surfaces of $t_{Mn\text{-}Ga}$ = 5 nm.

XRD patterns for $Mn_{62.0}Ga_{38.0}$ (at %) film of different thickness ($t_{Mn\text{-}Ga}$ nm) on MgO (100) substrate are shown in Fig.5. A fundamental peak, and superlattice peaks of the $L1_0$-MnGa phase were clearly observed for the $t_{Mn\text{-}Ga}$ = 100 nm. The $t_{Mn\text{-}Ga}$ = 20 nm film shows clear $L1_0$-MnGa (001), (002), (110) and (112) peaks (not shown (003)). The $t_{Mn\text{-}Ga}$ = 10 and 5 nm films show relatively small Mn-Ga (002), (110) and (112) peaks (not shown (001)). With decreasing thickness (100-5 nm), the Mn-Ga films show shift of diffraction angle (superlattice peaks are small). In addition, the chemical order parameter S of the $t_{Mn\text{-}Ga}$ = 20 nm film was shown S = 0.57, it shows a significant decrease in the S compared to the $t_{Mn\text{-}Ga}$ = 100 nm (S = 0.78).

Magnetization curves for $Mn_{62.0}Ga_{38.0}$ (at %) thin films of different thickness ($t_{Mn\text{-}Ga}$ nm) prepared on MgO (100) substrate are shown in Fig. 6. All measurements were preformed at room temperature. The magnetic field was

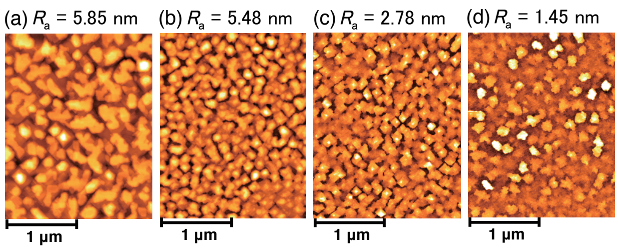

Fig. 7. AFM images for $Mn_{62.0}Ga_{38.0}$ (at %) thin films of different thickness ($t_{Mn\text{-}Ga}$ nm) prepared on MgO (100) substrate. $t_{Mn\text{-}Ga}$ of (a) 100, (b) 20, (c) 10 and (d) 5 at T_s = 300 ℃ and T_a = 300 ℃ (3 h).

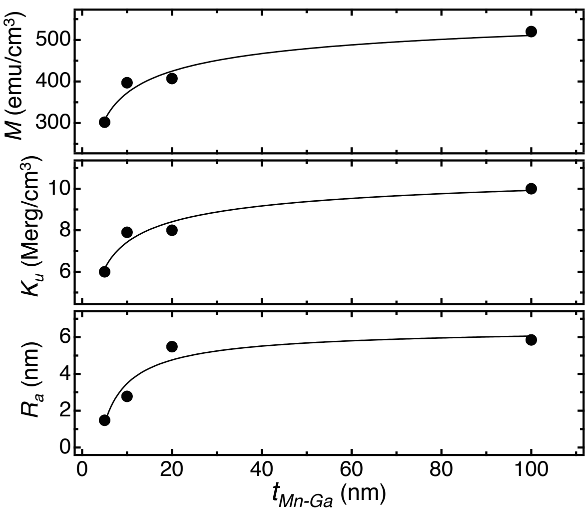

Fig. 8. M_s, K_u and R_a as function of $t_{Mn\text{-}Ga}$ (nm) for $Mn_{62.0}Ga_{38.0}$ (at %) thin films prepared on MgO (100) substrate at T_s = 300 ℃, T_a = 300 ℃ (3 h).

applied in the perpendicular (⊥) and in-plane (//) directions to the film. The easy magnetization axis is aligned perpendicular to the film plane for all the samples. With decreasing thickness (100-5 nm), M_s (= 520-302 emu/cm^3) and K_u (10.0-6.01 Merg/cm^3) were decreased. It can be considered that decreasing M_s and K_u originated primary from the decreased of chemical order parameter S. Furthermore, AFM images for $Mn_{62.0}Ga_{38.0}$ (at %) thin films of different thickness ($t_{Mn\text{-}Ga}$ nm) prepared on MgO (100) substrate are shown in Fig. 7. The average roughness (R_a) for the Mn-Ga surfaces ($t_{Mn\text{-}Ga}$ = 100, 20, 10 and 5 nm) was found to be R_a = 5.25, 4.74, 2.52 and 1.33 nm, respectively. With decreasing thickness (100-5 nm), R_a (= 5.25-1.33 nm) was decreased. The M_s, K_u and R_a as function of $t_{Mn\text{-}Ga}$ (nm) for Mn-Ga thin films are summarized in Fig.8. Considering that the growth temperature of PMA film should be as low possible for practical applications in spintronic devices, the $L1_0$-Mn-Ga highly oriented thin film is very promising because high PMA can be obtained at relative low growth temperature at T_s = 300 ℃ and T_a = 300 ℃ in this study.

4. Summary

Mn-Ga thin films have been fabricated by using UHV-EB vapor deposition and their magnetic properties were investigated. Variation of Mn composition has been confirmed by number of deposition. The clear oriented growth of Mn-Ga films has been confirmed on MgO (001) substrate by using RHEED in real time. Large M_s of 470 emu/cm^3 and K_u of 10.5 Merg/cm^3 were obtained for $L1_0$-Mn-Ga highly oriented thin film. With decreasing the thickness (100-5 nm), M_s (= 302 emu/cm^3), K_u (= 6.01 Merg/cm^3) and R_a (= 1.45 nm) were decreased. The $L1_0$-Mn-Ga highly oriented thin film is considered to be promising because relative high K_u and low M_s can be obtained at relatively low growth temperature at T_s = T_a = 300 ℃.

Acknowledgements This work was supported in part by the Ministry of Education, Culture, Sports, Science and Technology project for the "Hi-Tech Research Center Preparation Program" and performed at the Hi-tech Research Center of Tohoku Gakuin University. Part of this work was supported by "Collaborative Research Based on Industrial Demand" program from Japan Science and technology Agency.

References

1) S. Mizukami, T. Kubota, F. Wu, X. Zhang, T. Miyazaki, H. Naganuma, M. Oogane, A. Sakuma, and Y. Ando: *Phys. Rev. B,* **85**, 014416 (2012).
2) F. Wu, S. Mizukami, D. Watanabe, H. Naganuma, M. Oogane, Y. Ando and T. Miyazaki: *Appl. Phys. Lett.,* **94**, 122503 (2009).
3) B. Balke, G. H. Fecher, J. Winterlik and C. Felser: *Appl. Phys. Lett.*, **90**, 152504 (2007).
4) H. Kurt, K. Rode, M. Venkatesan, P. Stamenov and J. M. D. Coey: *Phys. Rev. B*, **83**, 020405R (2011).
5) A. Köhler, I. Knez, D. Ebke, C. Felser and S. S. P. Parkin: *Appl. Phys. Lett.*, **103**, 162406 (2013).
6) S. Mizukami, A. Sakuma, A. Sugihara, T. Kubota, Y. Kondo, H. Tsuchiura and T. Miyazaki: *Appl. Phys. Express*, **6**, 123002 (2013).
7) A. Sugihara, K. Z. Suzuki, T. Miyazaki and S. Mizukami: *J. Appl. Phys.*, **117**, 17B511 (2015).A. Köhler, I. Knez, D. Ebke, C. Felser and S. S. P. Parkin: *Appl. Phys. Lett.*, **103**, 162406 (2013).
8) T. Kubota, S, Ouardi, S. Mizukami, G. H. Fecher, C. Felser, Y. Ando and T. Miyazaki: *J. Appl. Phys.*, **113**, 17C723 (2013).
9) A. Sugihara, S. Mizukami, Y. Yamada, K. Koike and T. Miyazaki: *Appl. Phys. Lett.*, **104**, 132404 (2014).
10) K. Z. Suzuki, R. Ranjbar, A. Sugihara, T. Miyazaki and S. Mizukami: *Jpn. J. Appl. Phys.*, **55**, 010305 (2016).
11) Q. L. Ma, T. Kubota, S. Mizukami, X. M. Zhang, H. Naganuma, M. Oogane, Y. Ando and T. Miyazaki: *Appl. Phys. Lett.*, **101**, 032402 (2012).
12) W. Y. Zhang, P. Kharel, S. Valloppilly, R. Skomski and D. J. Sellmyer: *J. Appl. Phys.*, **117**, 17E306 (2015).
13) H. Yoda, T. Kishi, T. Nagase, M. Yoshikawa, K. Nishiyama, E. Kitagawa, T. Daibou, M. Amano, N. Shimomura, S. Takahashi, T. Kai, M. Nakayama, H. Aikawa, S. Ikegawa, M. Nagamine, J. Ozeki, S. Mizukami, M. Oogane, Y. Ando, S. Yuasa, K. Yakushiji, H. Kubota, Y. Suzuki, Y. Nakatani, T. Miyazaki, and K. Ando: *Curr. Appl. Phys.*, **10**, e87 (2010).
14) H. Lee, H. Sukegawa, J. Liu, T. Ohkubo, S. Kasai, S. Mitani and K. Hoho: *Appl. Phys. Lett.*, **107**, 032403 (2015).
15) J. Winterlik, B. Bake, G. H. Fecher, M. C. M. Alves, F. Bernardi and J. Morais: *Phys. Rev. B*, **77**, 054406 (2008).
16) S. Mizukami, F. Wu, A. Sakuma, J. Walowski, D. Watanabe, T. Kubota, X. Zhang, H. Naganuma, M. Oogane, Y. Ando and T. Miyazaki: *Phys. Rev. Lett.*, **106**, 117201 (2011).
17) Z. Bai, Y. Cai, L. Shen, M. Yang, V. Ko, G. Han and Y. Feng: *Appl. Phys. Lett*, **100**, 022408 (2012).
18) M. Glas, D. Ebke, I. M. Imort, P. Thomas and G. Reiss: *J. Magn. Mater.*, **333**, 134 (2013).
19) M. Li, X. Jiang, M. G. Samant, C. Felser and S. S. P. Parkin: *Appl. Phys. Lett.*, **103**, 032410 (2013).
20) Y. Miura and M. Shirai: *IEEE Trans. Magn.*, **50**, 1400504 (2014).

Received Oct. 10, 2016; Revised Dec. 26, 2016; Accepted Mar. 06, 2017